OPERATING CHARACTERISTICS OF POROUS FLOATING – RING JOURNAL BEARINGS OPERATING WITH AN IMPROVED BOUNDARY CONDITIONS

Dr. Basim A. Abass
Lecturer Mech. Eng. Dept

Dr. Alaa' M. Hussan
Asst. Prof College of Engineering

Lekaa' Hameed
Asst. Lecturer Babylon University

.

ABSTRACT

The static characteristics of porous floating ring journal bearing under hydrodynamic lubrication condition when operating with an improved boundary conditions are theoretically analyzed. An isothermal finite bearing theory was adopted during this analysis. The effect of different parameters, namely, permeability, geometrical dimensions of the ring and the bearing are considered. It was assumed that oil is supplied through the outside diameter of the bearing under low supply pressure. The angular extent of the oil – film formed in journal – ring and ring – bearing oil films was obtained by applying the integral momentum equation at the leading edge of the oil – film to define the beginning of the oil extent. While, the continuity of flow across the trailing edge was used to define the end of the oil extent. Numerical results show that the bearing performance affected by different parameters namely, permeability, eccentricity ratios of inner and outer oil – film, the clearance ratios, and the radii ratios.

KEY WORDS

hydrodynamic lubrication, floating ring, porous oil bearings, improved boundary conditions, slip velocity effect.

الخلاصة

يتضمن هذا البحث دراسة نظرية للخصائص السكونية للمساند ذاتية التزييت ذات الحلقة العائمة. تم اعتماد نظرية الركائز المحددة الطول والتي تعمل تحت ظروف ثبوت درجة الحرارة لغرض أجراء هذه الدراسة. تم الأخذ بنظر الاعتبار تأثر أداء السند بعدد من المؤثرات(النفاذية, والشكل الهندسي للحلقة) و لضمان عمل الركيزة تحت الظروف الهيدروديناميكية فقد تم افتراض بان الركيزة تجهز بالزيت من القطر الخارجي للركيزة تحت ضغط تجهيز منخفض. لقد تم تحديد بداية ونهاية طبقة الزيت باستخدام معادلة الزخم التكاملية لتحديد بداية طبقة الزيت ومعادلة استمرارية الجريان لتحديد نهاية طبقة الزيت. لقد أظهرت نتائج الدراسة بان ضغطا سالبا يتولد قبل نهاية طبقة الزيت كما هو متوقع عند مقارنة النتائج مع تلك المنشورة لبعض الباحثين الذين عملوا على دراسة تصرف المساند ذاتية التزييت. كما وأظهرت النتائج بان أداء المسند يتأثر بمختلف العوامل وهي ضغط التجهيز, النفاذية, نسبة اللاتمركز, نسبة الخلوص, ونسبة أنصاف أقطار الحلقة.

INTRODUCTION

Over the past decades a considerable number of experimental and theoretical studies have been carried out to study the characteristics of the solid floating ring journal bearing. Isothermal fluid flow analysis assumes a constant lubricant viscosity had been made by Shaw and Nussdorfer (1947), Orcut and Ng (1968), Tanaka and Hori (1972), Rohde and Ezzat (1980), Li and Rohde (1981). An experimental investigation to the behaviour of floating ring journal bearing was carried out by Kettleborough as early as in (1954). He found that there are significant discrepancies between test data and predictions. Tatara (1969) noting that, over certain speed ranges and for high feed pressure, floating ring journal bearing operate in a stable mode. Dong and Zhao (1990), investigate the possibility of using the floating ring journal bearing in automotive application. They found that it is possible for floating ring bearings to be used in engines where the load non – stationary. Chong and Kim (2001), studied the operating characteristics of counter rotating floating ring journal bearings. It is theoretically confirmed that floating ring journal bearings can be used in counter rotating journal bearings. Andres and Kerth (2004) studied the thermal effect on the performance of the floating ring journal bearing for turbochargers application. It was found that the ring speed ratio decreases dramatically as shaft speed rises.

Lubrication performance characteristics of porous oil bearings (load capacity, friction coefficient, bearing temperature. etc.) have been the object of many recent investigations, Morgan and Cameron (1957); Rouleau (1963); Goldstein and Braun (1971); Cusano (1979); Reason and Dyer (1973); Prakash and Vij (1974). In the above investigations the half Sommerfeld condition was adopted. A theoretical and experimental work done by Kaneko et. al. (1994) shows that the oil film is formed mainly in the loaded part of the bearing and the angular extent of oil film is significantly smaller than that formed in a solid journal bearing even under hydrodynamic lubrication condition. Kaneko et. al. (1997) used an improved boundary conditions to obtain the angular position of leading a trailing ends of the oil film regions. They show that the negative pressure occur before the tailing end of the oil film region. Elsharkawy and Lotfi (2001) made an analysis to the hydrodynamic lubrication of porous bearings using a modified Brinkman – extended Darcy model. They found that the numerical model has been successfully predicting the experimental results of different researchers.

The angular extent of the oil – film formed in journal – ring and ring – bearing oil films is obtained by applying the integral momentum equation at the leading edge of the oil – film to define the beginning of the oil extent while, the continuity of flow across the trailing edge is used to define the end of the oil extent. The analysis of the bearing performance shows the occurrence of a negative film pressure before the trailing end of the oil – films region as expected when compared the results with the behaviour of porous bearings obtained by different workers.

So the purpose of this study is to analyze the steady state performance of porous floating ring journal bearing working under improved boundary conditions which are used to determine the leading and trailing edge of the oil films.

NUMERICAL ANALYSIS:

Model of the Porous Floating Ring Journal Bearing:

The porous floating ring journal bearing with the coordinate system used in this analysis can be shown in figure (1). The journal rotates with a constant angular velocity (ω_j) about its axis while the porous ring rotates with an enhanced angular velocity (ω_r) about its center. The porous bearing inserted into a solid housing having a circumferential groove in the middle. Lubricant oil at low supply pressure (P_s) is supplied to the groove in the middle.

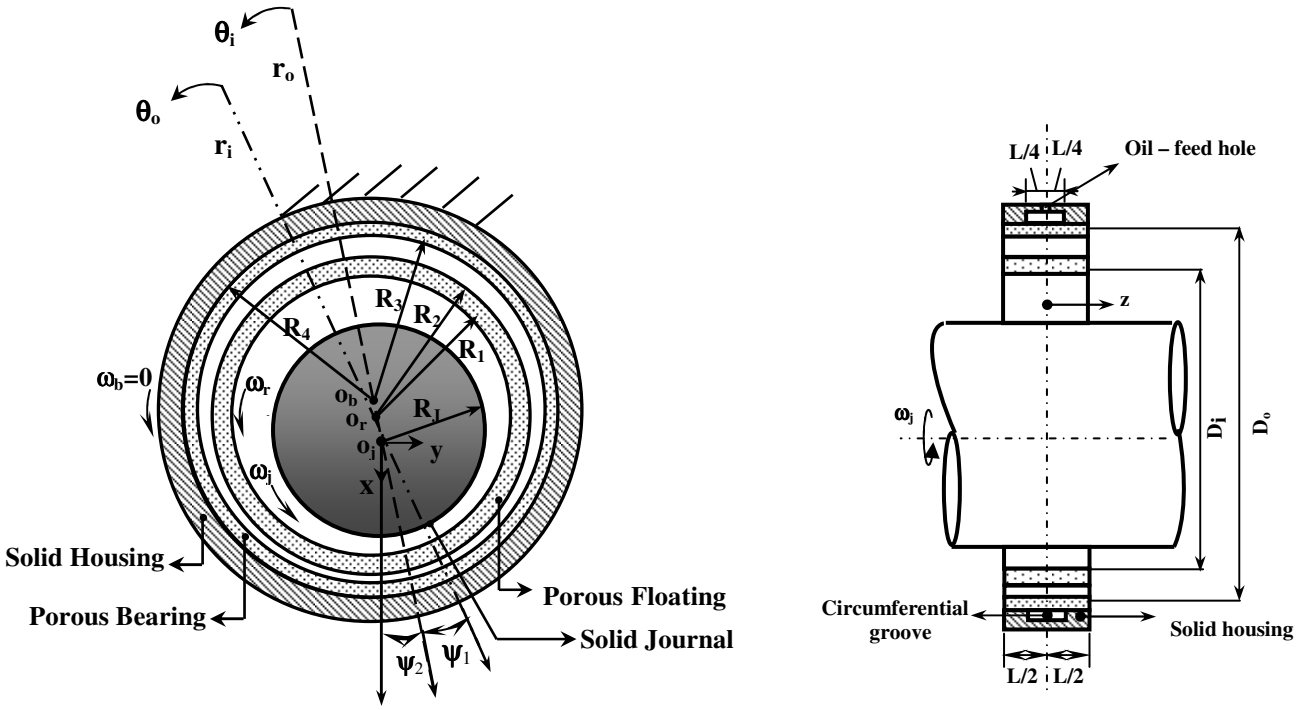

Fig. (1): Oil film region and oil flow of porous floating ring journal bearing

PRESSURE DISTRIBUTION IN OIL FILM AND POROUS MATRIX:

The performance of the bearing inner and outer oil films are obtained from the following Reynolds' equation for finite bearings including the so – called filter term and the effect of tangential slip velocity. For constant viscosity it can be written as, Kaneko et. al. (1997);

$$\frac{\partial}{\partial\theta}\left(h^{\wedge 3}(1+\zeta_1)\frac{\partial P^{\wedge}}{\partial\theta}\right)_{ii}+\left(\frac{D_{ii}}{L}\right)^2\frac{\partial}{\partial Z^{\wedge}}\left(h^{\wedge 3}(1+\zeta_1)\frac{\partial P^{\wedge}}{\partial Z^{\wedge}}\right)_{ii}=6\frac{\partial}{\partial\theta}\left(h^{\wedge 3}(1+\zeta_0)\right)_{ii}-12\Phi_{ii}\left(\frac{\partial P^{\wedge *}}{\partial r^{\wedge}}\Big|_{r^{\wedge}=1}\right)_{jj} \quad (1)$$

$$(\zeta_0)_{ii}=\left(\frac{s}{(h^{\wedge}+s)}\right)_{ii} \quad (2)$$

$$(\zeta_1)_{ii}=\left(3\left(h^{\wedge}s+2\alpha^2s^2\right)/\left\{h^{\wedge}(h^{\wedge}+s)\right\}\right)_{ii} \quad (3)$$

$$(s)_{ii}=\left(\Phi c/R\right)_{ii}^{1/2}/\alpha \quad (4)$$

$$(\Phi)_{ii}=(k_1R/c^3)_{ii} \quad (5)$$

$$\left(h^{\wedge}\right)_{ii}=h_{ii}/c_{ii}=(1+\varepsilon\cos(\theta))_{ii} \quad (6)$$

The slip coefficient (α) is a dimensionless parameter which depends on the porous material. In the present analysis a value of (0.1) is assumed for (α) as done in the pervious studies, Cusano (1979); Quan and Wang (1985); Kaneko et. al. (1994).

Oil pressure in the porous ring and porous bearing is governed by the Darcy's equation which can be written in dimensionless form as follows Kaneko et. al. (1997);

$$\frac{1}{r_{\hat{i}i}}\frac{\partial}{\partial \hat{r}}\left(\hat{r}\,\frac{\partial \hat{P}^{*}}{\partial \hat{r}}\right)_{jj}+\frac{1}{\hat{r}_{ii}^{2}}\left(\frac{\partial^{2}\hat{P}^{*}}{\partial^{2}\theta}\right)_{jj}+\left(\frac{D_{ii}}{L}\right)^{2}\left(\frac{\partial^{2}\hat{P}^{*}}{\partial^{2}\hat{Z}^{2}}\right)_{jj}=0 \qquad \textbf{(7)}$$

BOUNDARY CONDITIONS:

Two types of boundary conditions were used during this work.

OIL FILM PRESSURE BOUNDARY CONDITIONS:

The following boundary conditions were used to evaluate the pressure distribution through the oil films.

$$\left.\begin{aligned}
&\hat{P}\left(\theta_1,\hat{z}\right)_{ii}=\hat{P}^{*}\left(\hat{r},\theta_1,\hat{z}\right)_{ii}=0\\
&\hat{P}\left(\theta_2,\hat{z}\right)_{ii}=\hat{P}^{*}\left(\hat{r},\theta_2,\hat{z}\right)_{ii}=0\\
&\hat{P}\left(\theta,\pm1\right)_{ii}=\hat{P}^{*}\left(\hat{r},\theta,\pm1\right)_{ii}=0\\
&\hat{P}\left(\theta,z\right)_{ii}=\hat{P}^{*}\left(\hat{r},\theta,z\right)_{ii}\ \text{ at }\ \left(\hat{r}\right)=1\\
&\frac{\partial \hat{P}\left(\theta,0\right)}{\partial \hat{Z}}=\frac{\partial \hat{P}^{*}\left(\theta,\hat{r},0\right)}{\partial \hat{Z}}=0
\end{aligned}\right\} \qquad \textbf{(8)}$$

The outer surface of porous matrix consists of two parts as shown in figure (1),the first is the part press – fitted inside the solid housing, where the pressure is evaluated from the condition that the permeability of the housing adjacent to the porous matrix is zero i.e.;

$$\Phi=0 \quad \text{or} \quad \frac{\partial \hat{P}^{*}}{\partial \hat{r}}\ ;\ \text{at}\ \left(\hat{r}\right)_2\geq\left(r_o/r_i\right)_2\ \text{and}\ 0.5\leq\left|\hat{Z}\right|\leq1 \qquad \textbf{(9)}$$

The second is the part exposed to the circumferential groove in the housing, where the pressure is given by;

$$\left(\hat{P}^{*}\right)_2=\hat{P}_s=\frac{c_2^{2}P_s}{\left(r^{2}\eta\omega\right)_2}\quad \text{at}\quad \left(\hat{r}\right)_2\quad \text{and}\quad \left|\hat{Z}\right|\leq0.5 \qquad \textbf{(10)}$$

CIRCUMFERENTIAL BOUNDARY CONDITIONS:

The following boundary conditions are used to determine the oil film extent. The leading edge (θ_1) of the both oil films can be determined by extending the boundary condition used by Kaneko et. al. (1997), as follows;

$$\left(M_{\theta 1} - M_{\theta 2} - M_{\theta c} - M_{\theta b} \right)_{ii} = 0 \qquad \textbf{(11)}$$

where;

$M_{\theta_1}, M_{\theta 2}, M_{\theta c}$ and $M_{\theta b}$ are the circumferential momentum flow rates across the control surfaces of the oil films, as shown in figure (2). The momentum flow rates are given as follows;

$$\left.\begin{aligned}
\left(M_{\theta_1}\right)_{ii} &= 2\int_0^{L/2}\int_0^{(h_{\theta_1})_{ii}} \rho\left[\left(u_\theta|_{\theta_1}\right)^2\right]_{ii} dydz \\
\left(M_{\theta_2}\right)_{ii} &= 2\int_0^{L/2}\int_0^{(h_{\theta_1})_{ii}} \rho\left[\left(u_\theta|_{\theta_2}\right)^2\right]_{ii} dydz \\
\left(M_{\theta_c}\right)_{ii} &= 2(r_{ii})\int_{\theta_1}^{\theta_2}\int_0^{(h)_{ii}} \rho\left[\left(u_\theta * u_z\right)|_{z=L/2}\right]_{ii} dyd\theta \\
\left(M_{\theta_b}\right)_{ii} &= 2(r_{ii})\int_0^{L/2}\int_{(\theta_1)_{ii}}^{(\theta_2)_{ii}} \rho\left[\left(u_{\theta_m}\right)_{ii} * \left(u_r^*\right)_{jj}\right]_{r=(r)_{ii}} d\theta dz
\end{aligned}\right\} \qquad \textbf{(12)}$$

The velocity components $(u_\theta)_{ii}$ and $(u_z)_{ii}$ represent the components of the oil velocity in circumferential and axial directions in the both oil films, while $(u_r^*)_{jj}$ represents the radial velocity component of the oil inside the porous bearing and the porous ring. The values of $(\theta_1)_{ii}$ and $(\theta_2)_{ii}$ are assumed to be constant in z – direction.

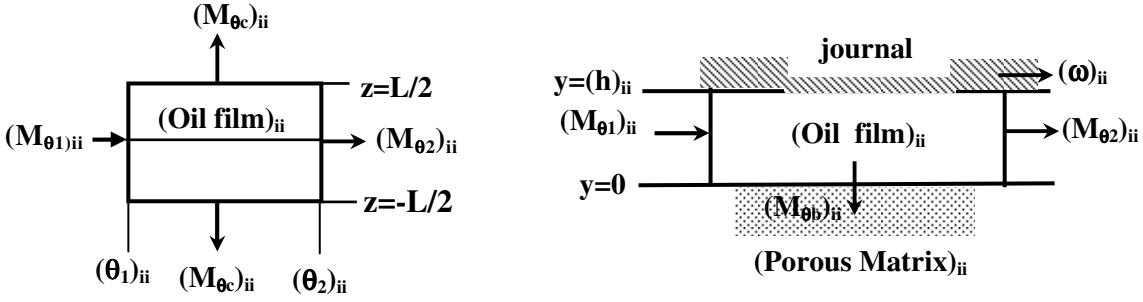

Fig. (2): Circumferential momentum flow rates

On the other hand the oil film extent at the trailing edge (θ_2) can be obtained by ensuring the continuity of the bulk flow a cross the boundary line at (θ_2).

$$\left(q_{\theta_p} / q_{\theta_c}\right)_{ii} = 0 \tag{13}$$

where q_{θ_p} and q_{θ_c} are the flow rates a cross the trailing boundary line due to the Poiseuilles' flow and due to the Couettes' flow respectively. Equation **(13)** can be rewritten as;

$$\left(q_{\theta_p} / q_{\theta_c}\right)_{ii} = \left(\left(\frac{(1+\zeta_1)}{6(1+\zeta_0)} h^{\wedge 2} \int_0^1 \frac{\partial P^{\wedge}}{\partial \theta} dz^{\wedge} \right)_{\theta=\theta_2} \right)_{ii} \tag{14}$$

Knowing the values of $(\theta_1)_{ii}$ and $(\theta_2)_{ii}$ for each oil film (journal – ring and ring – bearing oil films)**,** the angular extent of the first and second oil films $(\beta)_{ii}$ are expressed in the form;

$$(\beta)_{ii} = (\theta_2)_{ii} - (\theta_1)_{ii} \tag{15}$$

BEARING PARAMETERS:

Knowing the pressure distribution the dimensionless film force components along and perpendicular to the line of centers can be obtained, respectively as;

$$\left(\hat{W}_R\right)_{ii} = -\int_0^1 \int_{\theta_1}^{\theta_2} \left(P^{\wedge}(\theta, z)_{ii} \cos\theta\right)_{ii} d\theta dz^{\wedge} \tag{16}$$

$$\left(\hat{W}_T\right)_{ii} = \int_0^1 \int_{\theta_1}^{\theta_2} \left(P^{\wedge}(\theta, z)_{ii} \sin\theta\right)_{ii} d\theta dz^{\wedge} \tag{17}$$

the total dimensionless load can be expressed as;

$$\left(\hat{W}\right)_{ii} = \sqrt{\left(\hat{W}_R\right)_{ii}^2 + \left(\hat{W}_T\right)_{ii}^2} \tag{18}$$

The attitude angle $(\Psi)_{ii}$ can be evaluated as;

$$(\Psi)_{ii} = \tan^{-1}\left(W_T^{\wedge} / W_R^{\wedge}\right)_{ii} \tag{19}$$

The friction force on the inner and outer surfaces of the ring can be evaluated as;

$$F_{r_{ii}}^{\wedge} = \int_0^1 \int_{\theta_1}^{\theta_2} \pm \frac{h_{ii}^{\wedge}}{2} \frac{\partial P_{ii}^{\wedge}}{\partial \theta} d\theta dz^{\wedge} + \int_0^1 \int_{\theta_1}^{\theta_2} \frac{h_{ii}^{\wedge}}{2} \frac{\zeta_{1\theta}}{3} \frac{\partial P_{ii}^{\wedge}}{\partial \theta} d\theta dz^{\wedge} + \int_0^1 \int_{\theta_1}^{\theta_2} \frac{(1+\zeta_{0\theta})}{h_{ii}^{\wedge}} d\theta dz^{\wedge} \tag{20}$$

Hence the coefficient of friction can be evaluated as ;

$$\left(\mu^{\wedge}\right)_{ii} = \frac{\left(F_r^{\wedge}\right)_{ii}}{\left(\hat{W}\right)_{ii}} \tag{21}$$

STEADY STATE PERFORMANCE:

To calculate the steady state performance of the bearing it is necessary to find out the steady state equilibrium position of the journal and ring centers, the following conditions for moments and forces are hold for equilibrium state.

$$T_{inner}^{\wedge} = T_{outer}^{\wedge} \tag{22}$$

where,

$$T_{ii}^{\wedge} = \int_0^1 \int_{\theta_1}^{\theta_2} \pm \frac{h_{ii}^{\wedge}}{2} \frac{\partial P_{ii}^{\wedge}}{\partial \theta} d\theta dz^{\wedge} + \int_0^1 \int_{\theta_1}^{\theta_2} \frac{h_{ii}^{\wedge}}{2} \frac{\zeta_{1\theta}}{3} \frac{\partial P_{ii}^{\wedge}}{\partial \theta} d\theta dz^{\wedge} + \int_0^1 \int_{\theta_1}^{\theta_2} \frac{\left(1+\zeta_{0\theta}\right)}{h_{ii}^{\wedge}} d\theta dz^{\wedge} \tag{23}$$

The second equilibrium conditions which specify the steady state performance of the bearing is the force balance which state that;

$$W_1^{\wedge} = W_2^{\wedge} \tag{24}$$

The ring speed to the journal speed can be found from the torque equilibrium as follows;

$$\frac{N_r}{N_j} = \frac{T_{inner}^{\wedge}}{T_{outer}^{\wedge}} * \frac{R_1^3}{R_2^3} * \frac{c_2}{c_1} \tag{25}$$

METHOD OF SOLUTION:

Oil film pressure distribution and the oil pressure distribution through the porous matrix can be obtained by solving equations **(1)** and **(7)** simultaneously. These equations are discretized and solved simultaneously with an appropriate boundary conditions. In the present analysis **(180)** divisions in circumferential direction **(N_1),** divided into **(100)** divisions for the rupture zone and **(80)** divisions for the effective zone. Sixteen divisions in axial direction **(N_2)** and eight divisions in radial direction **(N_3)** have been adopted. The governing equations are transformed to discrete form using finite difference technique and then solved iteratively with successive under relaxation factor, to obtain the pressure and the location of the inlet and trailing boundary lines for the oil – film regions, the iterations are continued until the following inequalities are satisfied simultaneously,

$$\left(\frac{\sum\sum\sum \left| P_{i,j,k}^{\wedge^*(n+1)} - P_{i,j,k}^{\wedge^*(n)} \right|}{\sum\sum\sum \left| P_{i,j,k}^{\wedge^*(n)} \right|} < 10^{-5} \right)_{jj} \tag{26}$$

$$\left(\frac{\sum\sum \left| P_{j,k}^{\wedge(n+1)} - P_{j,k}^{\wedge(n)} \right|}{\sum\sum \left| P_{j,k}^{\wedge(n)} \right|} < 10^{-5} \right)_{ii} \tag{27}$$

$$\left(\left| M_{\theta_1}^{\wedge} - M_{\theta 2}^{\wedge} - M_{\theta c}^{\wedge} - M_{\theta_b}^{\wedge} \right| / M_{\theta_1}^{\wedge} < 10^{-3} \right)_{ii} \tag{28}$$

$$\left(\left| q_{\theta_p} / q_{\theta_c} \right| \right)_{ii} = \left(\left| \left(\frac{(1+\zeta_1)}{6(1+\zeta_0)} h^{\wedge 2} \int_0^1 \frac{\partial P^{\wedge}}{\partial \theta} dz^{\wedge} \right)_{\theta=\theta_2} \right| < 10^{-3} \right)_{ii} \tag{29}$$

To ensure the steady state performance of the bearing, the following equilibrium conditions must be satisfied;

- torque equilibrium :

$$\left| T_{inner} - T_{outer} \right| < 10^{-3} \tag{30}$$

- load equilibrium :

$$\left| W_1^{\wedge} - W_2^{\wedge} \right| < 10^{-3} \tag{31}$$

Always (n) and (n+1) used in above equations denote two consecutive iterations and the points i, j, k represent the grid number in radial, circumferential, and axial directions respectively.

where;

$$\left(\hat{M}_{\theta_1} \right)_{ii} = \left(M_{\theta_1} \right)_{ii} / \left(\rho c_{ii} r_{ii}^2 \omega_{ii}^2 L \right) = \int_0^1 \left(\left(\frac{h^{\wedge 5}}{1080} \left(\frac{\partial P^{\wedge}}{\partial \theta} \right)^2 \left(9 + 15\zeta_1 + 10\zeta_1^2 \right) \right)_{\theta=\theta_1} \right)_{ii} dZ^{\wedge}$$

$$- \int_0^1 \left(\left(\frac{h^{\wedge 3}}{36} \frac{\partial P^{\wedge}}{\partial \theta} \left(3 + 3\zeta_0 + 2\zeta_1 + 4\zeta_0\zeta_1 \right) \right)_{\theta=\theta_1} \right)_{ii} dZ^{\wedge} + \int_0^1 \left(\left(\frac{h^{\wedge}}{3} \left(1 + \zeta_0 + \zeta_0^2 \right) \right)_{\theta=\theta_1} \right)_{ii} dZ^{\wedge}$$

$$\left(\hat{M}_{\theta 2}\right)_{ii} = (M_{\theta 2})_{ii} / \left(\rho c_{ii} r_{ii}^2 \omega_{ii}^2 L\right) = \int_0^1 \left(\left(\frac{h^{\wedge 5}}{1080} \left(\frac{\partial P^{\wedge}}{\partial \theta} \right)^2 \left(9 + 15\zeta_1 + 10\zeta_1^2\right) \right)_{\theta=\theta 2} \right)_{ii} dZ^{\wedge}$$

$$- \int_0^1 \left(\left(\frac{h^{\wedge 3}}{36} \frac{\partial P^{\wedge}}{\partial \theta} \left(3 + 3\zeta_0 + 2\zeta_1 + 4\zeta_0\zeta_1\right) \right)_{\theta=\theta 2} \right)_{ii} dZ^{\wedge} + \int_0^1 \left(\left(\frac{h^{\wedge}}{3} \left(1 + \zeta_0 + \zeta_0^2\right) \right)_{\theta=\theta 2} \right)_{ii} dZ^{\wedge}$$

$$\left(\hat{M}_{\theta_c}\right)_{ii} = (M_{\theta c})_{ii} / \left(\rho c_{ii} r_{ii}^2 \omega_{ii}^2 L\right) = -\frac{1}{72} \left(\left(\frac{D}{L} \right)^2 \int_{\theta_1}^{\theta_2} A d\theta \right)_{ii}$$

(32)

$$\left(A = h^{\wedge 3} \left(3 + 3\zeta_0 + 2\zeta_1 + 4\zeta_0\zeta_1\right) \left. \frac{\partial P^{\wedge}}{\partial Z^{\wedge}} \right|_{Z^{\wedge}=1} \right)_{ii} \le 0 \qquad \text{if} \qquad \left(\left. \frac{\partial P^{\wedge}}{\partial Z^{\wedge}} \right|_{Z^{\wedge}=1} \right)_{ii} \le 0$$

$$A = 0 \quad \text{if} \quad \left(\left. \frac{\partial P^{\wedge}}{\partial Z^{\wedge}} \right|_{Z^{\wedge}=1} \right)_{ii} > 0$$

$$\left(\hat{M}_{\theta_b}\right)_{ii} = (M_{\theta b})_{ii} / \left(\rho c_{ii} r_{ii}^2 \omega_{ii}^2 L\right) = \int_0^1 \left(\int_{\theta_1}^{\theta_2} B d\theta \right)_{ii} dZ^{\wedge}$$

$$(B)_{ii} = \left(\Phi \left\{ \frac{h^{\wedge 2}}{12} \left(1 + \zeta_1\right) \frac{\partial P^{\wedge}}{\partial \theta} - \frac{1}{2} \left(1 + \zeta_0\right) \right\} \right)_{ii} \left(\left. \frac{\partial P^{\wedge *}}{\partial r^{\wedge}} \right|_{r^{\wedge}=1} \right)_{jj} \qquad \text{if} \qquad \left(\left. \frac{\partial P^{\wedge *}}{\partial r^{\wedge}} \right|_{r^{\wedge}=1} \right)_{jj} \le 0$$

$$(B)_{ii} = \left(\left(\frac{c}{r} \right) \Phi^2 \frac{\partial P^{\wedge}}{\partial \theta} \right)_{ii} \left(\left. \frac{\partial P^{\wedge *}}{\partial r^{\wedge}} \right|_{r^{\wedge}=1} \right)_{jj} \qquad \text{if} \qquad \left(\left. \frac{\partial P^{\wedge *}}{\partial r^{\wedge}} \right|_{r^{\wedge}=1} \right)_{jj} > 0$$

RESULTS AND DISCUSSION:

Figures (3-a) and (3-b) represents a comparison between the results obtained using the computer program which prepared and written in FORTRAN – 90 language and executed on a personal computer (Pentium 4) of 256MB Ram, through this work with that obtained from the published data in Kaneko et., al., (1997). The solution of porous floating ring journal bearing merely consists of parallel solutions of two ordinary porous bearings via the mobility method it can be shown that the average percentage of error evaluated is (2%).

Figure (4) shows that the oil film has a higher peak of pressure as the supply pressure increases, which can be attributed to the higher flow of oil out of the porous matrix. The oil film pressure increases with increasing the supply pressure and clearance ratio and decreasing the radii ratio as shown in figures (4,5,6). An increased oil film extent has been shown in this case.

The correlation between (ε_1) and (ε_2) can be shown in Figure (7 and 8). It is clear that (ε_1) some times become greater than (ε_2) and vice versa. This correlation affected by different

parameter, namely, permeability, clearance ratio and radii ratio. This is true to maintain the equilibrium condition of the bearing and to ensure that the bearing is hydrodynamically lubricated.

The correlation between the ring – bearing and the journal – ring eccentricity ratios is affected by the radii ratio as shown in Figure (9). It is clear that the ring – bearing eccentricity ratio becomes lower than the journal – ring eccentricity ratio for a bearing with a ring of radii ratio is less than (1.25) while, the ring – bearing eccentricity ratio become greater than the journal – ring eccentricity ratio for a ring with a radii ratio grater than (1.25). This is true to maintain the steady state performance of the bearing. Also the ring speed becomes greater as the radii ratio decreases which make (ε_1) greater than (ε_2) in this case.

The oil films extent increases with increasing values of the permeability as shown in figures (10 and 11). This is can be explained by knowing that the oil flow from the porous matrix increases in this case.

The coefficient of friction increases with higher values of permeability of the porous matrix as shown in figures (12 and 13). The values of the Sommerfeld number which give the minimum friction decreases with decreasing the values of the permeabilities.

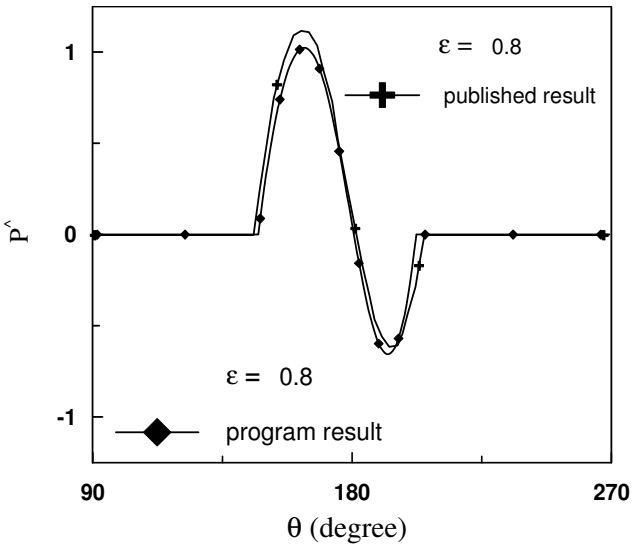

Fig. (3 -a), Comparison Between Experimental Published Results Kaneko, 1997with the Results obtained in the Present Work for Pressure Distribution at $P^{\wedge}_S = 0.1$.

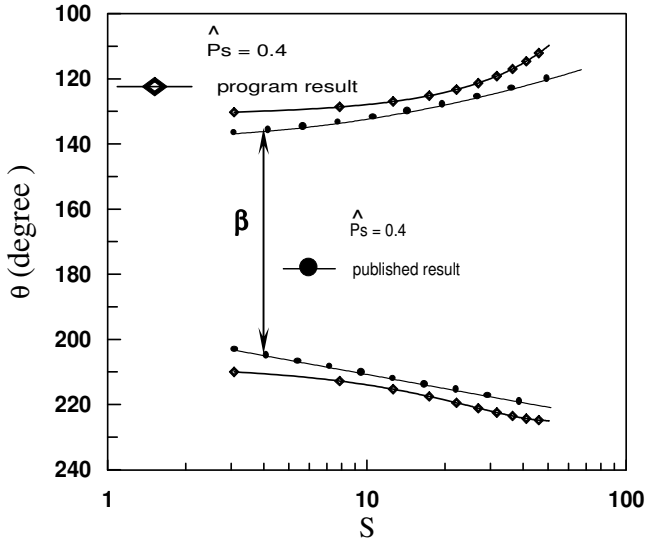

Figure (3 -b), Comparison Between Published Results [18] with the Results obtained in the Present Work for Oil – Film Extent.

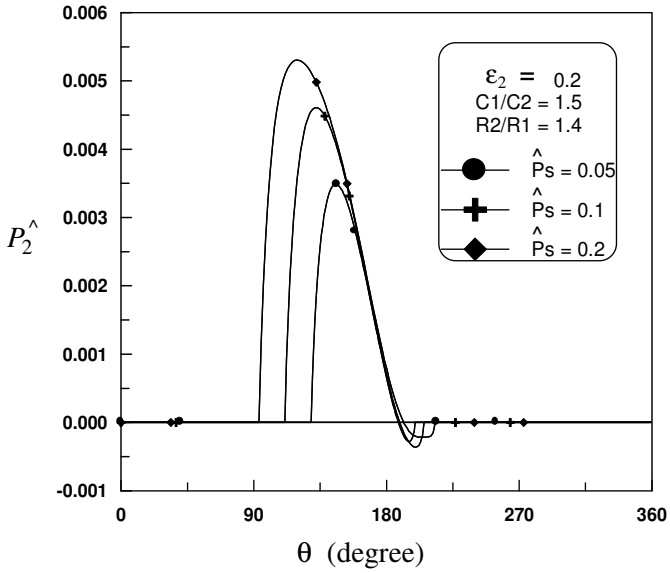

Fig. (4), Computed Results for Circumferential Pressure Distribution in Ring - Bearing Clearance Gap for Various Values of Dimensionless Oil – Feed Pressure.

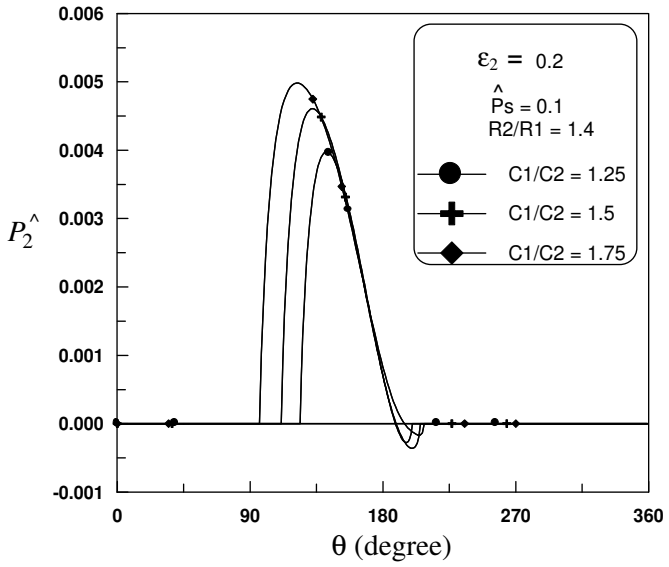

Fig. (5), Circumferential Pressure Distribution in Ring – Bearing Clearance Gap for Various Values of Clearance Ratios.

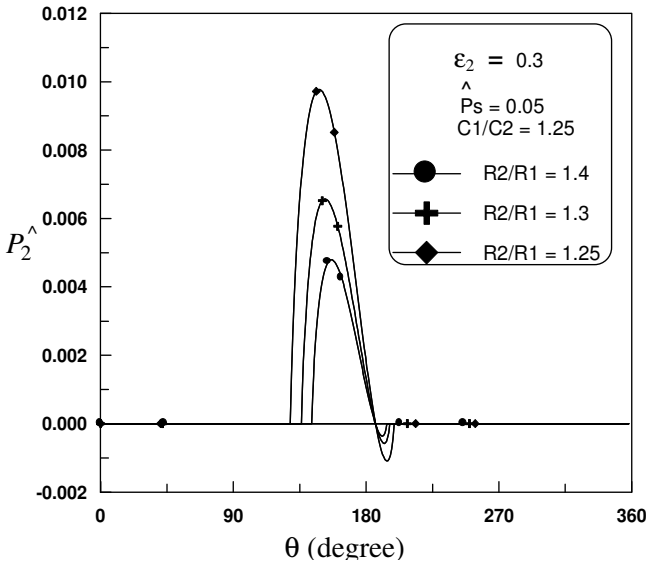

Fig. (6), Circumferential Pressure Distribution in Ring – Bearing Clearance Gap for Different Values of Radii Ratios.

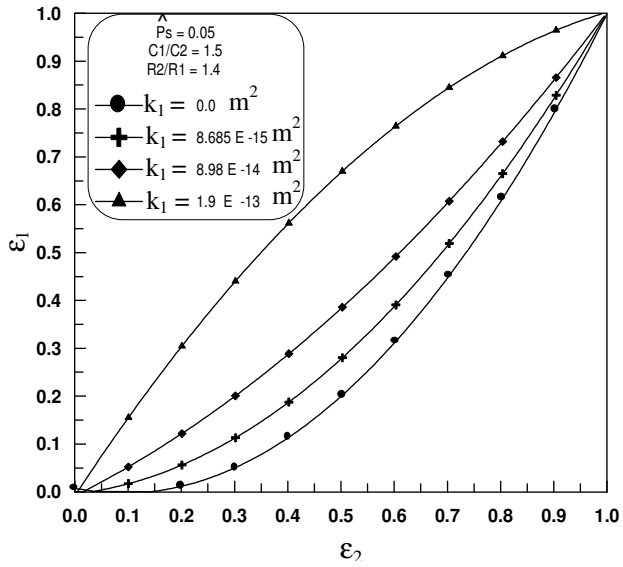

Fig. (7), Correlation Between Journal Eccentricity Ratio (ε_1) and Ring Eccentricity Ratio (ε_2) for Different Values of Permeability.

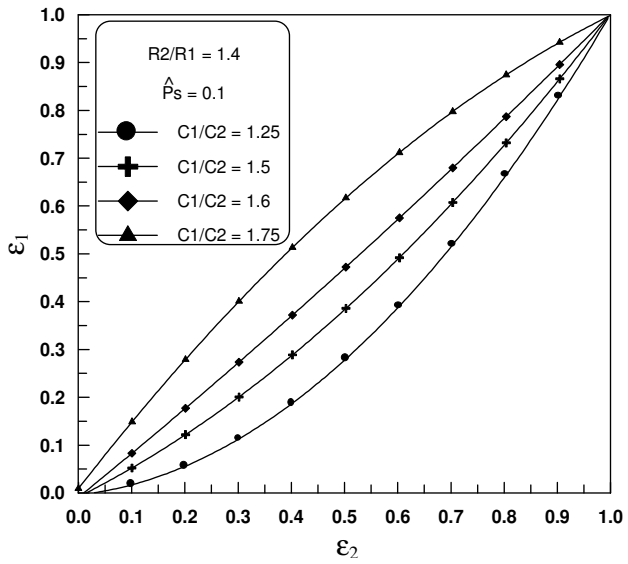

Fig. (8), Correlation Between Journal Eccentricity Ratio (ε_1) and Ring Eccentricity Ratio (ε_2) for Different Values of Clearance Ratio.

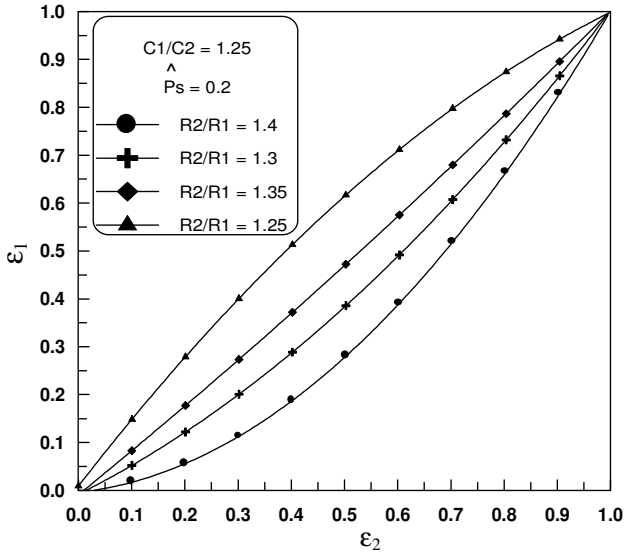

Fig. (9), Correlation Between Journal Eccentricity Ratio (ε_1) and Ring Eccentricity Ratio (ε_2) for Different Values of Radii Ratio.

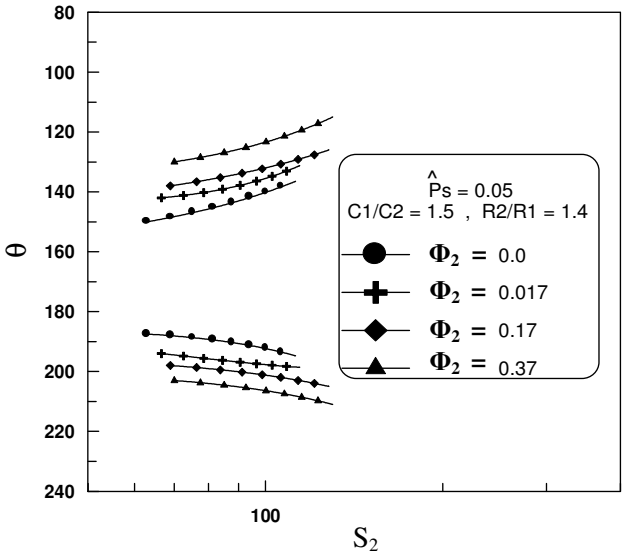

Fig (10), Outer Oil – Film Extent Versus Sommerfeld Number for Various Values of permeability parameter.

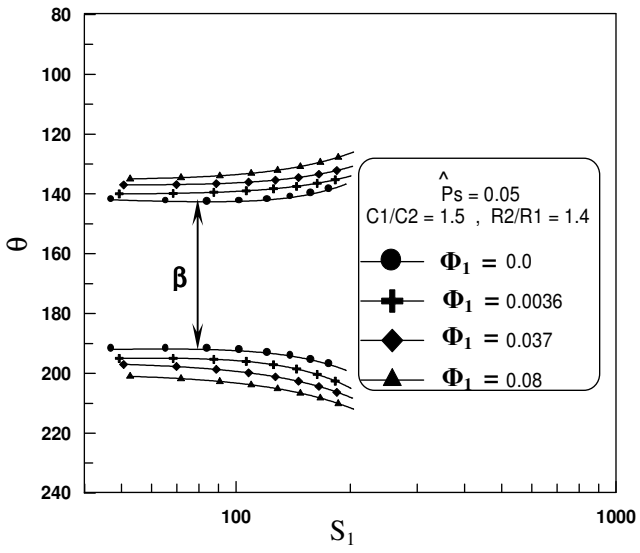

Fig. (11), Inner Oil – Film Extent Versus Sommerfeld Number for Various Values of permeability parameter.

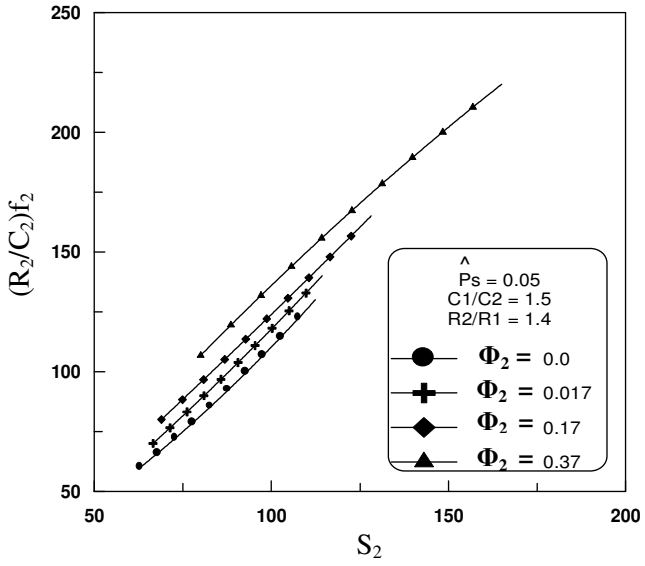

Fig. (12), Friction Coefficient of Outer Oil – Film Versus Sommerfeld Number for Different Values of Permeability Parameter.

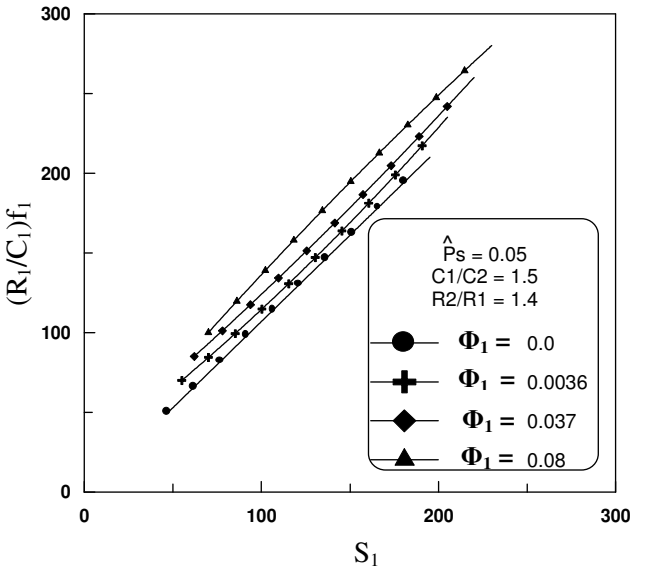

Fig. (13), Friction Coefficient of Inner Oil – Film Versus Sommerfeld Number for Different Values of Permeability Parameter.

CONCLUSIONS:

From the previous analysis the following can be concluded;

1- The load carrying capacity increases with increasing the values of the supply pressure and clearance ratio.

2- The load carrying capacity increases for the floating ring journal bearing working with ring has lower radii ratio.

3- The journal – ring eccentricity ratio become higher than the ring – bearing eccentricity ratio for bearings of higher permbility, clearance ratio and lower radii ratio.

4- The oil – film extent increases with decreasing the values of the ring radii ratio.

5- The minimum coefficient of friction decreases with increasing the values of the supply pressure and the clearance ratio. The minimum value of the friction coefficient decreases with decreasing the values of the radii ratio.

REFERENCES:

Abdallah A., Elsharkawy, Lotfi H., Guedouar, 2001, "Hydrodynamic Lubrication of Porous Journal Bearing Using a Modified Brinkman-Extended Darcy Model", Tribology International (34), July, pp. 767-777.

Andres, L. San, and Kerth, J., 2004, "Thermal Effect on the Performance of Floating Ring Bearings for Turbochargers", Proc. Instri. Mech. Engrs., Part J., J. Engineering Tribology, vol. 218, pp.437 – 450.

Cusano, C., 1979, "An analytical Study of Starved Porous Bearings", Transactions of the ASME, January, vol. 101, pp. 38 – 47.

Dong, X., and Zhao, Z., 1990, "Experimental and Analytical Research on Floating – Ring Bearing for Engine Applications", Journal of Tribology, January, vol. 112, pp. 119 – 122.

Goldstein, M. E., and Braun, W, H., 1971, "Effect of Velocity Slip at a Porous Boundary on the Performance of an Incompressible Porous Bearing." NASA Technical Note TN D-6181.

Kaneko, S., Ohkawa, Y., Hashimoto, Y., 1994, "A Study of Mechanism of Lubrication in Porous Journal Bearings: Effect of Dimensionless Oil –Feed Pressure on Static Characteristics Under Hydrodynamic Lubrication Conditions", Transactions of the ASME, July, vol. 116, pp. 606 – 610.

Kaneko, S., Hashimoto, Y., and Hiroki, I., 1997, "Analysis of Oil – Film Pressure Distribution in Porous Journal Bearings Under Hydrodynamic Lubrication Conditions Using An Improved Boundary Condition", Journal of Tribology, January, vol. 119, pp. 171 – 177.

Kettleborough, C. F., 1954, "Frictional Experiments on Lightly – Loaded Fully Floating Ring Journal Bearing", Aust. J. of App. Sci., January, pp. 211 – 219.

Li, C. H., and Rohde, S. M., 1981, "On the Steady State and Dynamic Performance Characteristics of Floating Ring Bearings", ASME Journal of Lubrication Technology, July, vol. 103, pp. 389 – 397.

Morgan, V. T., and Cameron, A., 1957, "Study of the Design Criteria for Porous Metal Bearings", Conference on Lubrication and Wear, Institution of Mechanical Engineers, London, paper No. 88, pp. 405 – 408.

Orcutt, F. K., and Ng. C.W. 1968, "Steady – State and Dynamic Properties of the Floating Ring Journal Bearing", ASME Journal of Lubrication Technology, vol. 90, pp. 1 – 10.

Prakash, J., and Vij, S., K., 1974, "Analysis of Narrow Porous Journal Bearing Using Beavers – Joseph Criterion of Velocity Slip", Transaction of the ASME, June, pp. 348 – 354.

Quan Yong – Xin and Wang Pei – Ming, 1985, "Theoretical Analysis and Experimental Investigation of Porous Metal Bearing", Tribology International, April, vol. 18, No. 2, pp. 67 – 73.

Reason, B. R., and Dyer, D., 1973, "A Numerical Solution for the Hydrodynamic Lubrication of Finite Porous Journal Bearings." Proceedings of the Institution of Mechanical Engineers, vol. 187, pp. 71-78.

Rohde, S. M., and Ezzat, M. A., 1980, "Analysis of Dynamically Loaded Floating Ring Bearing for Automotive Application", ASME Journal of Lubrication Technology, July, vol. 102, pp. 271 – 276.

Rouleau, W. T., 1963, "Hydrodynamic lubrication of Narrow Press-Fitted Porous Metal Bearing," ASME Journal of Basic Engineering, vol., 85 pp. 123-128.

Shaw, M. C., and Nussdorfer, Jr., T. J., 1947, "An Analysis of the Full Floating Journal Bearing", NACA Report, No. 866.

Tanaka, M. and Hori, Y., 1972, "Stability Characteristics of Floating Bush Bearings", ASME Journal of Lubrication Technology, July, vol. 94, pp. 248-259.

Tatara, A., 1969, "Vibration Suppressing Effect of Floating Bush Bearings", Journal of ASME vol., 72, pp. 1564-1569.

Yeon – Min Cheong and Kyung – Wood Kim, 2001, "Operating Characteristics of Counter – rotating Floating Ring Journal Bearings", KSTLE International Journal, December, vol. 2, No. 2, pp. 127 – 132.

NOMENCLATURE:

The following symbols are used throughout this work.

c_1 Journal – Ring Mean Radial Clearance (m)
c_2 Ring – Bearing Mean Radial Clearance (m)
$(h\hat{})_{ii}$ Dimensionless Film Thickness,$(h\hat{}=h/c)_{ii}$
$(k_1)_{jj}$ Permeability of the Porous Matrix (m^2)
L Length of the Ring and the Bearing Length (m)
$(M_{\theta 1})_{ii}$ Circumferential Momentum Flow Rate across Oil Film Surface at Inlet End of Oil – Film Region, i.e. at $(\theta = \theta_1)_{ii}$
$(M\hat{}_{\theta 1})_{ii}$ Dimensionless Circumferential Momentum Flow Rate across Oil – Film Surface at Inlet End of Oil–Film Region, i.e. at $(\theta = \theta_1)_{ii}$,$(M\hat{}_{\theta 1}= M_{\theta 1}/(\rho c(R*\omega)^2L)_{ii}$
$(M_{\theta 2})_{ii}$ Circumferential Momentum Flow Rate across Oil – Film Surface at Trailing End of Oil – Film Region, i.e. at $(\theta = \theta_2)_{ii}$
$(M\hat{}_{\theta 2})_{ii}$ Dimensionless Circumferential Momentum Flow Rate across Oil – Film Surface at Trailing End of Oil–Film Region, i.e. at $(\theta=\theta_2)_{ii}$, $(M\hat{}_{\theta 2}=M_{\theta 2}/(\rho c(R*\omega)^2L)_{ii}$
$(M_{\theta c})_{ii}$ Circumferential Momentum Flow Rate across Oil–Film Surface at Both Axial Ends($z= \pm L/2$)
$(M\hat{}_{\theta c})_{ii}$ Dimensionless Circumferential Momentum Flow Rate across Oil – Film Surface at Both Axial Ends i.e. at $(z = \pm L/2)$, $(M\hat{}_{\theta c}= M_{\theta c}/(\rho c(R*\omega)^2L)_{ii}$
$(M_{\theta b})_{ii}$ Circumferential Momentum Flow Rate across Oil – Film Surface Adjacent to Inner Surface of Ring and Bearing, i.e. (y=0)
$(M\hat{}_{\theta b})_{ii}$ Dimensionless Circumferential Momentum Flow Rate across Oil – Film Surface Adjacent to Inner Surface of Ring and Bearing , i.e. (y=0), $(M\hat{}_{\theta c}= M_{\theta c}/(\rho c(R*\omega)^2L)_{ii}$
N_j Journal Rotational Speed (r.p.m)
N_r Floating Ring Rotational Speed (r.p.m)
$(P\hat{})$ Dimensionless Oil-Film Pressure,$(P\hat{}=c^2P/(R^2\eta\omega))_{ii}$
$(P\hat{}^*)$ Dimensionless Oil – Film Pressure Inside the Porous Matrix,$(P\hat{}^*=c^2P^*/(R^2\eta\omega))_{jj}$
P_s Supply Pressure (N/m^2)
$r\hat{}$ Normalized radial coordinate, $r\hat{}= r/R_{ii}$
R_j Journal Radius(m)
(S) Sommerfeld Number , $(S= (R\eta\omega L / W)*(R / c)^2)_{ii}$
s Slip parameter
$T\hat{}$ Dimensionless Frictional Torque, $T\hat{} = T c / \eta\omega R^3L$
U_j Journal Velocity (m/s)
U_r Ring Velocity (m/s)
u,v,w Oil – Film Velocity Components in θ,r,z Directions Respectively(m/s)
u^*,v^*,w^* Oil Velocity Components inside the Porous Matrix in θ,r,z Directions Respectively (m/s)
$(W\hat{})$ Dimensionless Load Carrying Capacity, $(W\hat{})_{ii}=(W c^2 / \eta\omega R^3L)_{ii}$
$(W\hat{}_r)$ Dimensionless Component of Oil – Film Force Along the Line of Centers,
$(W\hat{}_T)$ Dimensionless Component of Oil – Film Force Perpendicular to the Line of Centers
$Z\hat{}$ Normalized axial coordinate, $Z\hat{}= z/(L/2)$

Greek Symbols

$(\varepsilon)_{ii}$ Eccentricity Ratio
η Absolute Viscosity of Oil(pa . s)
θ Angular Coordinate from Maximum Film Thickness Position (Degree)
$(\mu\hat{})_{ii}$ Dimensionless Friction Coefficient $(\mu\hat{})_{ii} = ((R/c)\mu)_{ii}$
ρ Density of oil (kg/m^3)
$(\Phi)_{ii}$ Permeability parameter, $(\Phi)_{ii} = (k_1 R / c^3)_{ii}$
$(\psi)_{ii}$ Attitude Angle (degrees)

Subscript

b Referring to Bearing
ii =1 referred for Journal – Ring Oil – Film
=2 referred for Ring – bearing Oil – Film
jj =1 for Porous Matrix of Floating Ring
=2 for Porous Matrix of Bearing
j Referring to Journal